Syntheses, Structures, and Bonding of Heteropentametallic Clusters $[MCo_3(CO)_{12}\{\mu_3\text{-}M'(EPh_3)\}]$ (M = Fe or Ru; M' = Cu or Au; E = P or As): *X*-Ray Crystal Structures of $[RuCo_3(CO)_{12}\{\mu_3\text{-}M'(PPh_3)\}]$ (M' = Cu or Au)†

Pierre Braunstein* and Jacky Rose
Laboratoire de Chimie de Coordination, UA 416 CNRS, Universite Louis Pasteur, 4 rue Blaise Pascal, F-67070 Strasbourg Cédex, France
Alain Dedieu
Laboratoire de Chimie Quantique, ER 139 CNRS, Universite Louis Pasteur, 4 rue Blaise Pascal, F-67070 Strasbourg Cedex, France
Yves Dusausoy and Jean-Paul Mangeot
Laboratoire de Mineralogie et Cristallographie, UA 162 CNRS, Universite de Nancy 1, Boite Postale 239, F-54506 Vandoeuvre-les-Nancy Cedex, France
Antonio Tiripicchio and Marisa Tiripicchio-Camellini
Istituto di Chimica Generale ed Inorganica dell' Universita, Centro di Studio per la Strutturistica Diffrattometrica del C.N.R., Via M. D'Azeglio 85, I-43100 Parma, Italy

The cluster anions $[MCo_3(CO)_{12}]^-$ [M = Fe (**1**) or Ru (**2**)] react with $[\{Cu(PPh_3)Cl\}_4]$ in toluene to give the neutral pentametallic clusters $[FeCo_3(CO)_{12}\{\mu_3\text{-}Cu(PPh_3)\}]$ (**3**) and $[RuCo_3(CO)_{12}\{\mu_3\text{-}Cu(PPh_3)\}]$ (**4**). The latter two products react with PPh_3 to give the ionic cluster species $[Cu(PPh_3)_3][MCo_3(CO)_{12}]$. The pentametallic cluster $[RuCo_3(CO)_{12}\{\mu_3\text{-}Au(PPh_3)\}]$ (**5**), obtained by reaction of (**2**) with $Au(PPh_3)Cl$ in diethyl ether–toluene, also reacts with PPh_3 to give $[Au(PPh_3)_2][RuCo_3(CO)_{12}]$. The structures of (**4**) and (**5**) have been determined by *X*-ray methods. Crystals of (**4**) are monoclinic, space group $P2_1/m$, with $Z = 2$ in a unit cell of dimensions $a = 9.122(3)$, $b = 15.010(6)$, $c = 12.580(7)$ Å, and $\beta = 107.86(3)°$. Crystals of (**5**) are monoclinic, space group $P2_1/c$, with $Z = 4$ in a unit cell of dimensions $a = 8.921(3)$, $b = 14.165(2)$, $c = 26.72(1)$ Å, and $\beta = 91.95(4)°$. The structures have been solved from diffractometer data by Patterson and Fourier methods and refined by full-matrix least-squares to $R = 0.049$ and 0.058 for 1 329 and 1 994 observed reflections, respectively. Both structures consist of a trigonal bipyramid of metal atoms with the cobalt atoms occupying the triangular equatorial plane and the copper or gold and ruthenium atoms situated at the apices. Three carbonyl groups bridge the Co–Co edges; the other nine are terminal, three attached to the Ru atom and two to each Co atom. Similarities in the bonding relationships of (**4**) and (**5**) are analyzed and rationalized through extended Huckel calculations.

Until very recently, there were relatively few examples of mixed-metal carbonyl clusters containing copper or silver atoms directly bonded to transition metals.[1-4] This is surprising in view of the growing number of studies on related gold complexes.[5,6] Furthermore, mixed-metal clusters containing a Group 8 metal associated with copper, such as $[Ru_6C(CO)_{16}\{Cu(NCMe)\}_2]$, have been shown to be valuable catalysts for CO hydrogenation.[7] This catalytic relevance could become even more pronounced if more examples were known of clusters containing *two* different Group 8 metals associated with a Group 1B metal, in view of possible synergic effects. Gold-containing mixed-metal clusters are generally efficiently prepared by reaction of a preformed cluster anion with the appropriate mononuclear halogeno-complex AuLCl or its corresponding cation $[AuL]^+$. Since the cation $[ML]^+$ (M = Cu, Ag, or Au) does not donate an electron to the cluster, electron-counting rules predict no structural change in the metal-core geometry of the resulting cluster.[8] This has indeed been observed in all known cases but one,[9] although skeletal rearrangements of the final cluster have been reported.[10] On the other hand, extended Hückel molecular orbital calculations have shown that a co-ordinated CuL unit has better π-accepting properties than co-ordinated AuL, thus calling for experimental support.[11] It would therefore be interesting to extend the class of copper-containing mixed-metal clusters in order to evaluate these effects and allow comparisons between closely related systems.[3,12]

We have now prepared and characterized the new heteropentametallic clusters $[MCo_3(CO)_{12}\{\mu_3\text{-}Cu(EPh_3)\}]$ (M = Fe or Ru, E = P or As) and compare in the present paper the crystal structures of $[RuCo_3(CO)_{12}\{\mu_3\text{-}Cu(PPh_3)\}]$ (**4**) and $[RuCo_3(CO)_{12}\{\mu_3\text{-}Au(PPh_3)\}]$ (**5**). Preliminary results of the structure determination of (**5**) have been reported previously.[13]

Results and Discussion

The cluster anion $[RuCo_3(CO)_{12}]^-$ has recently been shown to react with diphenylacetylene, affording the butterfly cluster $[NEt_4][RuCo_3(CO)_{10}(C_2Ph_2)]$,[14] and with $Au(PPh_3)Cl$, affording the heteropentametallic cluster $[RuCo_3(CO)_{12}\{\mu_3\text{-}Au(PPh_3)\}]$ (**5**).[13] Depending on the work-up conditions, two different forms of (**5**) can be isolated in the solid state, which become identical in solution (see Experimental section).

† Tri-μ-carbonyl-1,1,2,2,3,3-hexacarbonyl-μ_3-tricarbonylruthenio-μ_3-triphenylphosphinecuprio-*triangulo*-tricobalt and tri-μ-carbonyl-1,1,2,2,3,3-hexacarbonyl-μ_3-tricarbonylruthenio-μ_3-triphenylphosphineaurio-*triangulo*-tricobalt respectively.

Supplementary data available (No. SUP 56371, 16 pp.): thermal parameters, full lists of bond lengths and angles, least-squares planes data, calculated H-atom co-ordinates for (**4**). See Instructions for Authors, *J. Chem. Soc., Dalton Trans.*, 1986, Issue 1, pp. xvii—xx. Structure factors are available from the editorial office.

Non-S.I. unit employed: eV ≈ 1.60×10^{-19} J.

This reaction has now been extended to the copper analogue and shown to apply equally to the $[FeCo_3(CO)_{12}]^-$ cluster [equation (i)].

$$K[MCo_3(CO)_{12}] + \tfrac{1}{4}[\{Cu(PPh_3)Cl\}_4] \longrightarrow (OC)_2Co(\mu\text{-}CO)_2Co(CO)_2 + KCl \quad (i)$$

(1) M = Fe
(2) M = Ru

(3) M = Fe
(4) M = Ru

The complexes were characterized by ^{31}P n.m.r., i.r., and u.v. spectra, and analytical data (see Experimental section) which indicate their similarities. Complexes (3) and (4) are analogous to $[RuCo_3(CO)_{12}\{\mu_3\text{-}Au(PPh_3)\}]$ (5), as shown by the comparison of their structures (see below).

Complexes (3) and (4) react with triphenylphosphine, leading to the ionic derivatives (6) and (7) [equation (ii)].

$$[MCo_3(CO)_{12}\{\mu_3\text{-}Cu(PPh_3)\}] + PPh_3 \longrightarrow \tfrac{2}{3}[Cu(PPh_3)_3][MCo_3(CO)_{12}] + \ldots \quad (ii)$$

M = Fe (6)
M = Ru (7)

Surprisingly, $[Cu(PPh_3)_2][MCo_3(CO)_{12}]$ was not observed in reaction (ii), nor found in reaction (iii), indicating the strong preference for the formation of $[Cu(PPh_3)_3]^+$.

$$K[RuCo_3(CO)_{12}] + [Cu(PPh_3)_2]NO_3 \longrightarrow (4) + (7) + KNO_3 + \ldots \quad (iii)$$
(2)

Similar observations [equation (iv)] were made with $AsPh_3$ instead of PPh_3, leading for example to the formation of (8) and (9) (see Experimental section).

$$2K[FeCo_3(CO)_{12}] + 2Cu(AsPh_3)_2Cl \longrightarrow [FeCo_3(CO)_{12}\{\mu_3\text{-}Cu(AsPh_3)\}] + [Cu(AsPh_3)_3][FeCo_3(CO)_{12}] + 2KCl \quad (iv)$$
(1) (8) (9)

In contrast, reaction of (5) with one equivalent of PPh_3 yielded quantitatively $[Au(PPh_3)_2][RuCo_3(CO)_{12}]$ (10) [equation (v)].

$$[RuCo_3(CO)_{12}\{\mu_3\text{-}Au(PPh_3)\}] + PPh_3 \longrightarrow [Au(PPh_3)_2][RuCo_3(CO)_{12}] \quad (v)$$
(5) (10)

Reactions (ii) and (v) clearly demonstrate the electrophilic character of the Group 1B metal centre. This is further shown by the behaviour of (4) or (5) in basic solvents such as tetrahydrofuran (thf) or acetone, in which they dissociate and liberate the anions (1) and (2) respectively. This must be kept in mind when measuring the i.r. spectra of such polar clusters in solution.

Crystal Structures of $[RuCo_3(CO)_{12}\{\mu_3\text{-}M'(PPh_3)\}]$ [M' = Cu (4) *or* Au (5)].—The crystal structures of (4) and (5) consist of discrete molecules separated by normal van der Waals distances. Views of the molecules of (4), which has an imposed C_s-*m* symmetry, and (5) are shown in Figures 1 and 2, respectively, together with atomic-numbering schemes. Selected bond distances and angles are given and compared in Table 1.

The $RuCo_3M'$ metal core is in a trigonal-bipyramidal arrangement with the Ru and M' atoms capping a triangle of Co atoms. The PPh_3 ligand is bound to the M' atom and of the nine terminal carbonyl groups, three are attached to the Ru atom and two to each Co atom. With regard to the three bridging carbonyls, in (4) one is perfectly symmetrical for imposed constrictions [Co(2)–C(8) = 1.98(2) Å] and two (related by mirror symmetry) are symmetrical [Co(1)–C(5) = 1.94(1) and

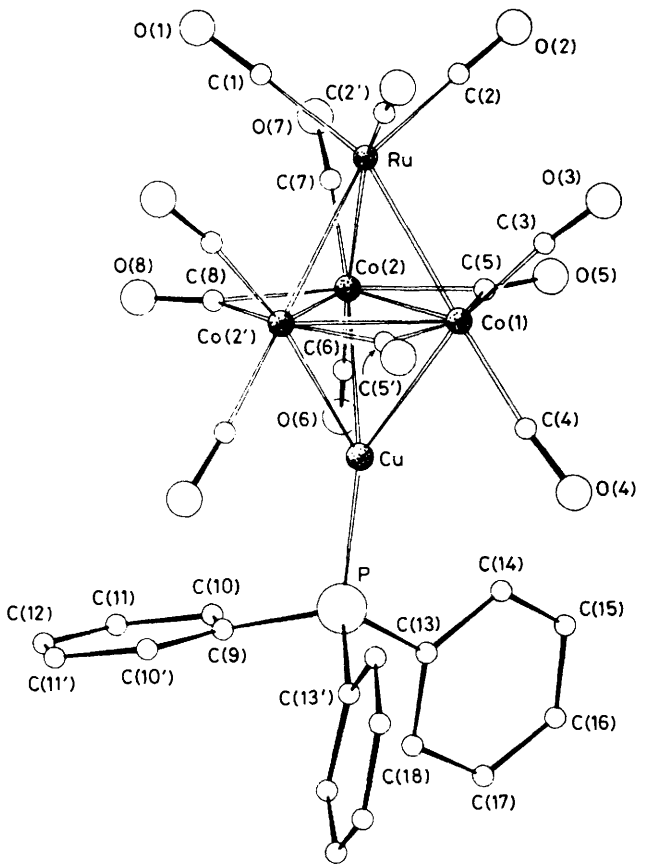

Figure 1. View of the molecule of $[RuCo_3(CO)_{12}\{\mu_3\text{-}Cu(PPh_3)\}]$ (4) showing the atomic-numbering scheme

Table 1. Comparison of selected bond distances (Å) and angles (°) for $[RuCo_3(CO)_{12}\{\mu_3\text{-}M'(PPh_3)\}]$ [M′ = Cu (**4**) or Au (**5**)]*

(4)		(5)		(4)		(5)	
Ru–Co(1)	2.631(3)	Ru–Co(1)	2.679(4)	Co(1)–Co(2)–Co(2′)	60.2(1)	Co(1)–Co(2)–Co(3)	60.6(1)
Ru–Co(2)	2.625(2)	Ru–Co(2)	2.664(4)	Co(2)–Co(1)–Co(2′)	59.7(1)	Co(2)–Co(1)–Co(3)	58.9(1)
		Ru–Co(3)	2.687(5)			Co(1)–Co(3)–Co(2)	60.5(1)
Co(1)–Co(2)	2.519(3)	Co(1)–Co(2)	2.539(6)	Co(1)–Ru–Co(2)	57.3(1)	Co(1)–Ru–Co(2)	56.7(1)
Co(2)–Co(2′)	2.507(2)	Co(2)–Co(3)	2.497(5)	Co(2)–Ru–Co(2′)	57.0(1)	Co(2)–Ru–Co(3)	55.6(1)
		Co(1)–Co(3)	2.543(6)			Co(3)–Ru–Co(1)	56.6(1)
Cu–Co(1)	2.551(4)	Au–Co(1)	2.745(4)	Co(1)–Cu–Co(2)	59.3(1)	Co(1)–Au–Co(2)	55.8(1)
Cu–Co(2)	2.538(2)	Au–Co(2)	2.679(4)	Co(2)–Cu–Co(2′)	59.2(1)	Co(2)–Au–Co(3)	54.9(1)
		Au–Co(3)	2.740(4)			Co(3)–Au–Co(1)	55.2(1)
Cu–P	2.203(5)	Au–P	2.287(6)	Co(1)–Cu–P	150.7(2)	Co(1)–Au–P	139.4(2)
Ru–C(1)	1.90(2)	Ru–C(1)	2.00(2)	Co(2)–Cu–P	142.1(1)	Co(2)–Au–P	153.1(2)
Ru–C(2)	1.92(1)	Ru–C(2)	1.94(3)			Co(3)–Au–P	148.8(1)
		Ru–C(3)	1.77(3)	Cu–P–C(9)	110.6(6)	Au–P–C(13)	110.6(7)
Co(1)–C(3)	1.77(2)	Co(1)–C(4)	1.79(3)	Cu–P–C(13)	115.2(4)	Au–P–C(19)	116.5(7)
Co(1)–C(4)	1.77(2)	Co(1)–C(5)	1.76(3)			Au–P–C(25)	113.5(8)
Co(1)–C(5)	1.94(1)	Co(1)–C(12)	1.86(3)	Ru–C(1)–O(1)	178(2)	Ru–C(1)–O(1)	171(3)
		Co(1)–C(6)	1.91(3)	Ru–C(2)–O(2)	178(2)	Ru–C(2)–O(2)	176(3)
Co(2)–C(5)	1.92(1)	Co(2)–C(12)	2.04(2)			Ru–C(3)–O(3)	174(3)
Co(2)–C(6)	1.77(1)	Co(2)–C(10)	1.84(3)	Co(1)–C(3)–O(3)	174(2)	Co(1)–C(4)–O(4)	169(3)
Co(2)–C(7)	1.76(1)	Co(2)–C(11)	1.71(3)	Co(1)–C(4)–O(4)	175(2)	Co(1)–C(5)–O(5)	173(2)
Co(2)–C(8)	1.98(2)	Co(2)–C(9)	2.03(2)	Co(1)–C(5)–O(5)	138(1)	Co(1)–C(12)–O(12)	149(2)
		Co(3)–C(6)	1.93(3)			Co(1)–C(6)–O(6)	137(2)
		Co(3)–C(7)	1.86(3)	Co(2)–C(5)–O(5)	141(1)	Co(2)–C(12)–O(12)	130(2)
		Co(3)–C(8)	1.72(3)	Co(2)–C(6)–O(6)	175(1)	Co(2)–C(10)–O(10)	169(3)
		Co(3)–C(9)	2.03(2)	Co(2)–C(7)–O(7)	172(1)	Co(2)–C(11)–O(11)	150(3)
P–C(9)	1.85(2)	P–C(13)	1.82(2)	Co(2)–C(8)–O(8)	141(1)	Co(2)–C(9)–O(9)	139(2)
P–C(13)	1.83(1)	P–C(19)	1.79(2)			Co(3)–C(6)–O(6)	139(2)
		P–C(25)	1.79(2)			Co(3)–C(7)–O(7)	171(3)
						Co(3)–C(8)–O(8)	166(3)
						Co(3)–C(9)–O(9)	145(2)

* Primed atoms are related to unprimed ones by mirror symmetry (transformation $x, \frac{1}{2} - y, z$).

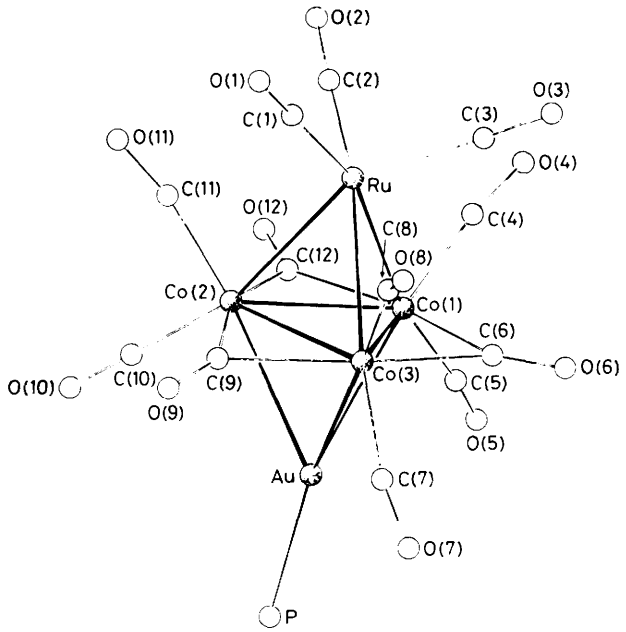

Figure 2. View of the molecule of $[RuCo_3(CO)_{12}\{\mu_3\text{-}Au(PPh_3)\}]$ (**5**) showing the atomic-numbering scheme

Co(2)–C(5) = 1.92(1) Å], whereas in (**5**), one is asymmetrical [Co(1)–C(12) = 1.86(3) and Co(2)–C(12) = 2.04(2) Å] and two symmetrical [Co(1)–C(6) = 1.91(3), Co(3)–C(6) = 1.93(3); Co(2)–C(9) = 2.03(2) and Co(3)–C(9) = 2.03(2) Å].

The structures of (**4**) and (**5**) are essentially similar and comparable with that of $[RuCo_3(CO)_{12}\{\mu_3\text{-}HgCo(CO)_4\}]$[15] in which the $HgCo(CO)_4$ fragment replaces the isoelectronic $M'(PPh_3)$ fragment. In these clusters the copper, gold, or mercury atoms may be considered as *sp* hybridized, one lobe pointing towards the centre of the Co_3 triangle. In (**4**) the Ru–Co bond distances [2.625(2) and 2.631(3) Å] are slightly shorter than in the gold complex (**5**) [2.664(4), 2.679(4), and 2.687(5) Å] and in the mercury complex [2.677(6), 2.686(5), and 2.686(5) Å]. The Cu–Co bond distances in (**4**) [2.538(2) and 2.551(4) Å] are longer than in $[\{CuCo(CO)_4\}_4]$ (in the range 2.360—2.372 Å),[16] the only other known Cu–Co distances reported to our knowledge. The Au–Co bond distances in (**5**) [2.679(4), 2.740(4), and 2.745(4) Å] are comparable (within 3σ) to the average value found in $[FeCo_3(CO)_{12}\{\mu_3\text{-}Au(PPh_3)\}]$ [2.714(7) Å],[17] but longer than in the bimetallic complex $[Co(CO)_4\{Au(PPh_3)\}]$ [2.50(1) Å].[18]

Only very few mixed-metal clusters have been structurally characterized which only differ by the nature of the Group 1B metal (*i.e.* Cu or Au).[3,19] Such systems are therefore particularly interesting to develop in order to enable an evaluation of the differences between the bonding modes of the CuL and AuL fragments. Indeed, it has been shown by Evans and Mingos[11] that for the $Au(PPh_3)$ fragment, the p_x and p_y orbitals are relatively high lying and cannot accept electron density as effectively as $Cu(PPh_3)$. We shall return to this point later in the discussion.

Despite obvious differences in the steric bulk of the Cu(NCMe) and $Au(PPh_3)$ groups, this bonding argument has been used to rationalize the interesting differences in the structures of the $[Os_{10}C(CO)_{24}(M'L)]^-$ clusters in which the Cu(NCMe) and $Au(PPh_3)$ fragments respectively cap an Os_3 face and bridge an Os_2 edge.[12] A similar situation has been

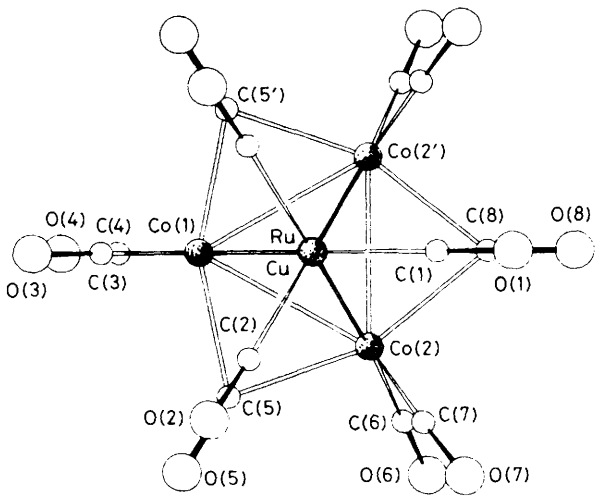

Figure 3. Projection of the molecule (**4**) in the Co_3 plane

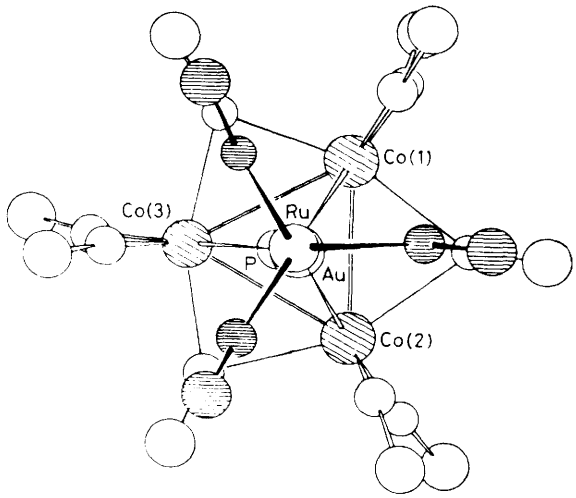

Figure 4. Projection of the molecule (**5**) in the Co_3 plane

found in $[Ru_6C(CO)_{16}(M'L)_2]$ (M' = Cu, L = MeCN; M' = Au, L = PPh_2Me).[20,21]

In our case, however, we find no significant difference in the bonding mode of the sterically comparable $Cu(PPh_3)$ and $Au(PPh_3)$ fragments in (**4**) and (**5**), respectively. Thus, in view of the different covalent radii of Cu (1.17 Å) and Au (1.34 Å),[22] the range spanned by the Cu–Co [2.538(2)—2.551(4) Å] and Au–Co [2.679(4)—2.745(4) Å] distances is not significantly different. The present bonding analysis (see below) accounts for this observation.

Figures 3 and 4 show projections of the $RuCo_3(CO)_{12}M'$ moieties of (**4**) and (**5**) on the Co_3 plane. It is interesting to compare the distances between the apical atoms and the Co_3 plane. Indeed the distances from the Cu and Au atoms to the Co_3 plane are 2.086(3) Å and 2.296(2) Å, respectively, quite comparable when corrected for the difference in covalent radii. In contrast, the distance between the Ru atom and this plane increases from 2.189(2) Å in (**4**) to 2.240(3) Å in (**5**). It appears therefore that a more covalently bonded M'L fragment (Au > Cu) induces an increased remoteness of the other apical atom in these trigonal-bipyramidal structures. This effect is even more pronounced when the d^{10} fragment is replaced by the yet more covalently-bonded $HgCo(CO)_4$.[15]

In (**4**), short Cu···C separations, involving copper and a carbonyl on each cobalt atom, are observed [Cu···C(4) = 2.58(2) and Cu···C(6) = 2.60(1) Å], without these carbonyls deviating appreciably from linearity. In $[PPh_3Me][Os_{10}C(CO)_{24}\{Cu(NCMe)\}]$[12] short Cu···C separations involving copper and three carbonyls [2.30(4), 2.40(3), and 2.46(6) Å] have been observed, and these carbonyls retained their linearity. Short Cu···C(carbonyl) distances [minimum value 2.471(5) Å] have also been found in $[Ru_6C(CO)_{16}\{Cu(NCMe)\}_2]$[20] but slight deviations from linearity of the carbonyls were observed.

In (**5**) for comparison, the Au···C separations involving C(5), C(7), and C(10) are 3.04(2), 2.98(2), and 2.90(3) Å, respectively, with Co–C–O angles ranging from 169(3) to 173(2)°. Taking into account the increased covalent radius of Au *vs.* Cu, these contacts are significantly longer than the corresponding Cu···C ones in (**4**). It is not clear whether the carbonyl distortions represent some degree of long-range interaction (attractive[12] or repulsive[20]) with the copper or gold atom, or result from steric effects in the solid. Relatively short non-bonding contacts between Cu^I or Au^I and C(carbonyl) atoms must be analyzed with caution.[20,23,24]

Since the angles at the cobalt atoms between the terminal carbonyls remain roughly constant within each molecule and also between (**4**) and (**5**), the greater Au···C non-bonding separations discussed above are reflected in Ru···C(4), Ru···C(8), and Ru···C(11) contacts [2.71(3), 2.84(3), 2.46(3) Å] in (**5**) shorter than the Ru···C(3) and Ru···C(7) contacts [2.89(2), 2.80(1) Å] in (**4**).

Theoretical Analysis.—The structural features described above call for a theoretical analysis of this type of cluster. There are other clusters which belong to this class, *e.g.* $[FeCo_3(CO)_{12}\{\mu_3\text{-}Au(PPh_3)\}]$[17] and $[FeCo_3H(CO)_9\{P(OCH_3)_3\}_3]$.[25] One would therefore like to unravel the bonding relationships of these systems, with two major goals in mind: (*i*) to assess the factors which account for their stabilization, and (*ii*) to rationalize on electronic grounds the *trans* influence observed on going along the series M' = $Cu(PPh_3)$, $Au(PPh_3)$, or $HgCo(CO)_4$ in the $RuCo_3(CO)_{12}M'$ systems.

We will base our discussion on extended Hückel calculations,[26] details of which are given in the Experimental section, using the fragment molecular orbital approach,[27] and also on perturbation theory arguments.

We start first by analyzing the bonding relationships in $[RuCo_3(CO)_{12}\{\mu_3\text{-}Au(PPh_3)\}]$ (**5**), using as a model of the triphenylphosphine ligand the PH_3 phosphine ligand. This system may be considered as three fragments, namely $Co_3(CO)_9^{3-}$, $Ru(CO)_3^{2+}$, and $Au(PH_3)^+$. Although this charge partitioning is somewhat arbitrary, it is nevertheless consistent with the actual relative ordering of the corresponding energy levels (see for instance Figure 8).

The $Co_3(CO)_6^{3-}$ moiety of the $Co_3(CO)_9^{3-}$ fragment is in fact analogous to a longitudinal Pt_3L_6 system (**I**). We[28] and others[29] have shown that, although being more stable than in the latitudinal (or planar) conformation (**II**), this system should not be very stable since it involves d^{10}–d^{10} interactions between ML_2 entities, all antibonding counterparts of the bonding

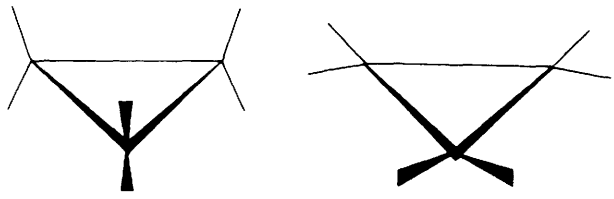

(I) (II)

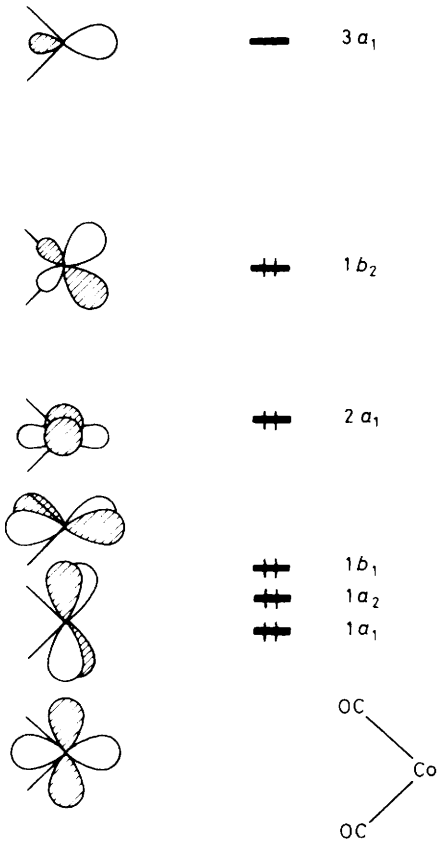

Figure 5. The valence orbitals of the $Co(CO)_2^-$ unit

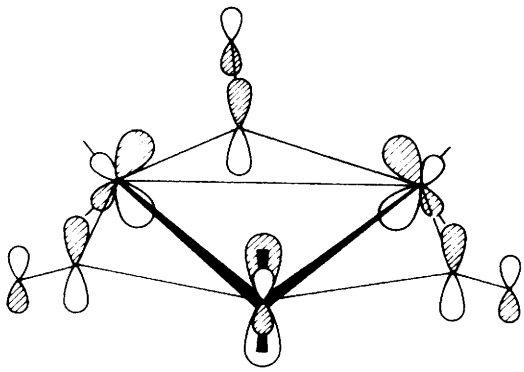

(III)

As shown in Figure 5, the $Co(CO)_2^-$ units are made up of a group of three orbitals which are almost degenerate ($1a_1$, $1a_2$, and $1b_1$ in the C_{2v} point group) below the $2a_1$ orbital, and a high lying $1b_2$ orbital which has been destabilized through antibonding interactions with the lone pair of the carbonyl ligands. Well above $1b_2$ (*i.e.* about 6 eV higher in energy) is a $3a_1$ or 'hy' *sp* hybrid orbital. When necessary in the following discussion, the orbitals of the $Co(CO)_2^-$ units will be indicated in parentheses. For instance the a''_2 combination (in D_{3h} symmetry) of the b_2 orbitals will be referred to as $a''_2(b_2)$.

There is an important factor which contributes to increase the total stability in the $Co_3(CO)_9^{3-}$ system. The three bridging carbonyl ligands provide a set of symmetry-adapted in-plane and out-of-plane† π^*_{CO} combinations which stabilize the corresponding combinations [namely $a''_2(b_2)$, $e'(2a_1)$, and $e''(a_2)$] of the $Co_3(CO)_6^{3-}$ moiety. This is shown for instance for the $a''_2(b_2)$ combination, (**III**).

On the other hand, some other levels of the $Co_3(CO)_6^{3-}$ moiety are destabilized through antibonding interactions with the proper symmetry combination of the n_{CO} lone pairs of the carbonyl ligands. This destabilization is partially offset, however, by a greater admixture of the *sp* hybrid combinations. This is especially true for the $a'_1(2a_1)$ combination as shown schematically in (**IV**). The net balance of these interactions is a positive one, *i.e.* the trinuclear system with 30 *d* electrons is stabilized through the interaction of the bridging carbonyl ligands.‡

The next step is therefore to assess the role of the capping systems, *i.e.* the $Ru(CO)_3^{2+}$ and $Au(PH_3)^+$ fragments. The corresponding valence orbitals are also well known[11,31b] and are shown in Figures 6 and 7 respectively. For $Ru(CO)_3^{2+}$ one finds, above a nest of three occupied orbitals $1a_1 + 1e$, three empty orbitals, hybridized away from the carbonyl ligands, the $2e$ and the $2a_1$ orbitals. The $Au(PH_3)^+$ fragment may be considered as being isolobal[11] to the $Ru(CO)_3^{2+}$ fragment. There is a noticeable difference however: the empty $3e$ set of $Au(PH_3)^+$ made up of the $6p_x$ and $6p_y$ orbitals, is much higher in energy than the $2e$ set of $Ru(CO)_3^{2+}$. In our calculations, the corresponding energies are -5.93 and -10.87 eV respectively.

The interaction pattern of these two fragments with the $Co_3(CO)_9^{3-}$ system is easy to understand. There are three primary interactions which account for the stabilization of the clusters (as shown in the simplified interaction diagram of Figure 8): the $2a_1$ orbitals of $Ru(CO)_3^{2+}$ and $Au(PH_3)^+$ can form an in-phase (**V**) and an out-of-phase (**VI**) combination which are both empty and which stabilize the $a'_1(2a_1)$ (**IV**) and the $a''_2(b_2)$ (**III**) combinations of the $Co_3(CO)_9^{3-}$ fragment. The stabilization is greater for the $a''_2(b_2)$ orbital, due to a greater overlap of this orbital with (**VI**): note that the lobes of (**III**) are directed toward the capping units. As far as the levels of *e* symmetry are concerned, there is a rather strong stabilizing interaction between the $e''(b_2)$ set of the $Co_3(CO)_9^-$ moiety and the $2e$ set of $Ru(CO)_3^{2+}$. The corresponding bonding

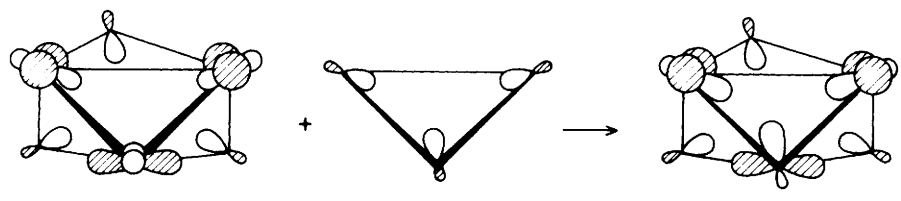

(IV)

interactions being filled. We shall not derive once again the bonding pattern of the 42-electron M_3L_6 system which is known.[28-30] We shall just, since we will make use of it later, recall briefly the orbitals of the three basic $Co(CO)_2^-$ units.[31]

† We refer here to the plane of the three cobalt atoms.

‡ The effect of the admixture of the *sp* hybrids is to reinforce the metal metal bonding.

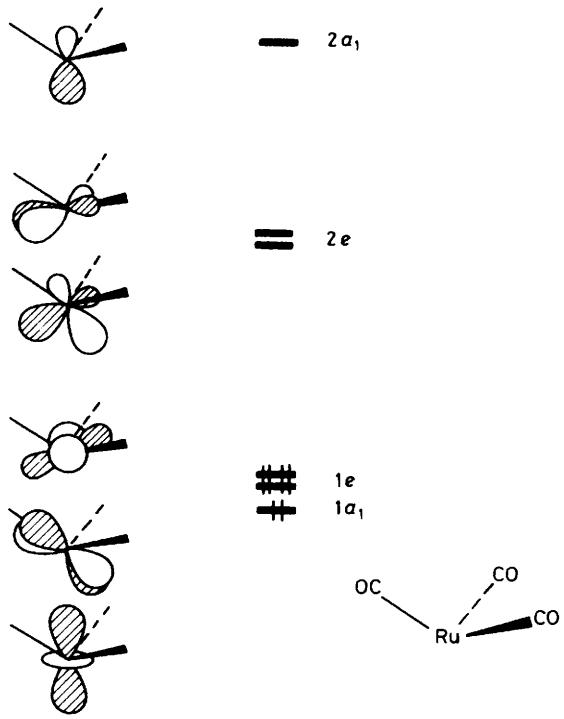

Figure 6. The valence orbitals of the $Ru(CO)_3^{2+}$ fragment

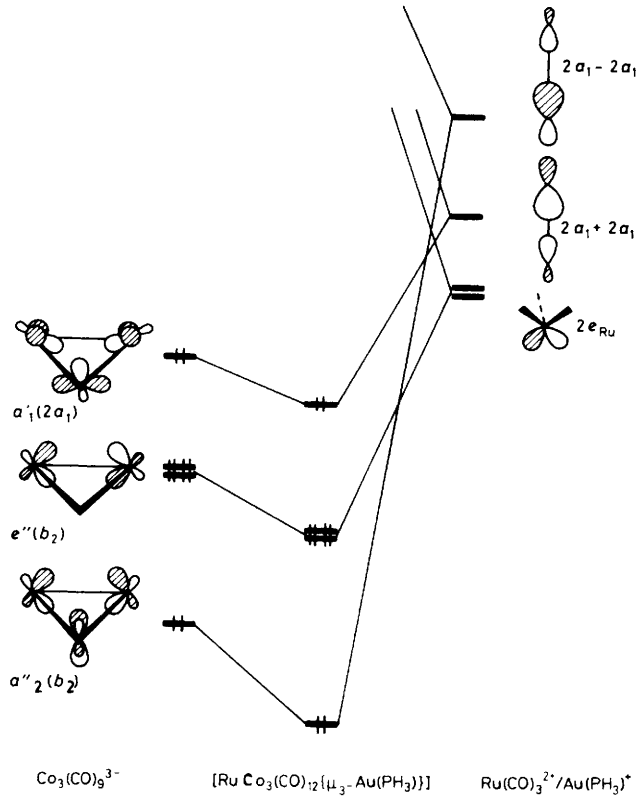

Figure 8. Simplified interaction diagram between the $Co_3(CO)_9^{3-}$ fragment and the $Ru(CO)_3^{2+}$ and $Au(PH_3)^+$ fragments to compose $[RuCo_3(CO)_{12}\{\mu_3\text{-}Au(PH_3)\}]$. Only the most interacting orbitals are shown

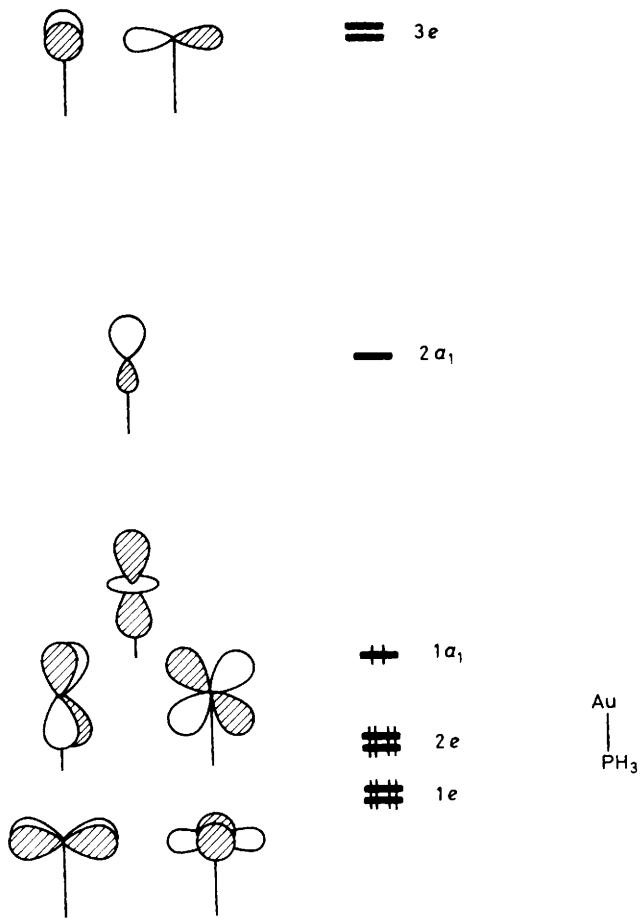

Figure 7. The valence orbitals of the $Au(PH_3)^+$ fragment

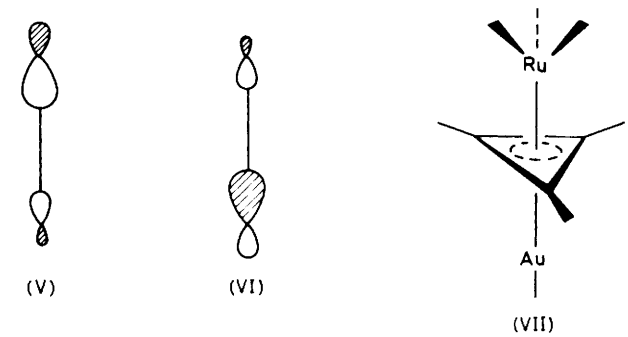

combination is somewhat destabilized, however, by an out-of-phase mixing of the occupied $2e$ set of $Au(PH_3)^+$. [We note here that the empty $3e$ levels of $Au(PH_3)^+$ do not mix significantly with the $e''(b_2)$ levels for energy reasons, since the energy gap is quite important (5.62 eV) and greater than the energy gap with the $2e$ $Au(PH_3)^+$ set, which amounts to 3.43 eV.]

At this stage, it is interesting to mention some points pertaining to this bonding pattern. The reader familiar with the isolobal analogy concept will have perhaps noticed that this system corresponds to an inverse sandwich structure. Since the main bonding interactions of the $Co_3(CO)_9^{3-}$ fragment arise from the $a''_2 + e''$ orbitals, this fragment can be considered as isolobal to the cyclopropenide anion $C_3H_3^{3-}$ and the whole system as isolobal to (**VII**).

It should be also noticed that the longitudinal conformation (**I**) of the Co_3L_6 moiety, which is imposed by the bridging

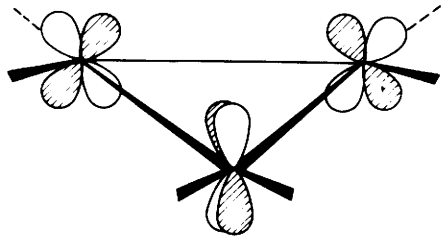

(VIII)

ligands, is more favourable for interaction with the capping units than the latitudinal conformation (**II**): in the latter the $a''_2(b_2)$ and $e''(b_2)$ orbitals involved in the bonding combinations with the capping units would not be hybridized away from the carbonyl ligands, see for instance (**VIII**), and would therefore have a smaller overlap with (**VI**) and the $2e$ set of $Ru(CO)_3^{2+}$. As a result, the expected stabilization would be lessened.

What about the effect of substituting $Au(PPh_3)$ by $Cu(PPh_3)$ or $HgCo(CO)_4$? A look at the corresponding interaction diagrams does not show any substantial difference along the series, and the bonding pattern is very similar in the three cases. More specifically, we do not find any interaction of importance between the $e''(b_2)$ levels of $Co_3(CO)_9^{3-}$ and the $3e$ empty levels of $Cu(PH_3)$. This is somewhat contradictory to the conclusion reached by Evans and Mingos.[11] In our case, the empty p_x and p_y levels are not significantly lower in energy in $Cu(PH_3)$ than in $Au(PH_3)$ (-6.33 *vs.* -5.93 eV).* This theoretical finding is in agreement with the experimental observation, quoted above, that the range spanned by the Cu–Co and Au–Co distances is not significantly different.

The lengthening of the Ru to Co_3 plane distance on going from (**4**) to (**5**) and to $[RuCo_3(CO)_{12}\{\mu_3\text{-}HgCo(CO)_4\}]$ still has to be understood. The rationale for this phenomenon lies in the consideration of the interactions for the orbitals of a'_1 symmetry, along the same lines followed by Burdett and Albright[32] in their analysis of the *trans* influence. These authors showed that the stabilization Δ_{ML} of the ML bond, when replacing one L ligand in the linear LML system by a L′ ligand, has the form of equation (vi), where S, S', $\Delta\varepsilon$, and $\Delta\varepsilon'$ are the

$$\Delta_{ML} \sim \frac{S^2}{\Delta\varepsilon} - \frac{S'^2}{\Delta\varepsilon'} \qquad \text{(vi)}$$

overlaps and the orbital energy differences between the metal orbital (d_{z^2}, p_z, or s) and the σ orbitals of the two ligands L and L′ respectively (provided that the concept of ligand additivity will apply). Hence, on varying the nature of L′, the ML stabilization energy decreases (and thus the ML bond length is expected to increase) with increasing $S'^2/\Delta\varepsilon'$. In the present case there are two stabilizing interactions involving the $2a_1$ orbitals of L = $Ru(CO)_3^{2+}$ and of L′ = $Cu(PH_3)^+$, $Au(PH_3)^+$, or $HgCo(CO)_4^+$: one with $a'_1(2a_1)$ and one with $a''_2(b_2)$. We shall add the two corresponding $S'^2/\Delta\varepsilon'$ terms,† the result of which is shown in Table 2. From this Table, the increase in the $\Sigma(S'^2/\Delta\varepsilon')$ term parallels the increase in the Ru to Co_3 plane distance along the series $Cu(PPh_3)$, $Au(PPh_3)$, $HgCo(CO)_4$. A closer examination of the $\Sigma(S'^2/\Delta\varepsilon')$ term indicates that the marked increase observed for $HgCo(CO)_4$ arises from a rather important decrease in the energy of the $2a_1$ level for $HgCo(CO)_4$ as compared to $Au(PH_3)$ (-10.129 *vs.* -8.529 eV). This low energy of the $2a_1$ orbital accounts for the more covalent character of the Hg to Co_3 interaction which we have mentioned (see above).

Table 2. Values of $\Sigma(S'^2/\Delta\varepsilon')$ (see text for definition) and the distance from the Ru atom to the Co_3 plane for the $RuCo_3(CO)_{12}M'$ systems of (**4**) and (**5**)

M′	$\Sigma\frac{S'^2}{\Delta\varepsilon'}$	Ru to Co_3 plane distance (Å)
$Cu(PH_3)$	0.0449	2.189(2) (this work)
$Au(PH_3)$	0.0456	2.240(3) (this work)
$HgCo(CO)_4$	0.0495	2.258(4)

Changing the $Au(PH_3)^+$ fragment to the proton H^+ should not alter the basic conclusions of this study since both systems are known to be isolobal. There may be concern about the possibility of having the proton inside the triangular Co_3 plane. A look at the orbital shapes of Figure 8 indicates that the stabilizing interaction with the $a'_1(2a_1)$ level would be increased, but that the stabilizing interaction with the $a''_2(b_2)$ would be decreased. Moreover, in order to relieve the steric effects (with a Co–Co distance of 2.53 Å, the Co–H distance would be 1.46 Å) the Co_3 triangle would have to expand to a rather significant extent. For the same Co–H distance as in $[FeCo_3H(CO)_9\{P(OCH_3)_3\}_3]$ (1.734 Å),[25] the Co–Co bond length would have to be 3.00 Å. Both arguments (orbitals and steric) therefore account for the proton capping the Co_3 face rather than sitting inside.‡

Experimental

Air-sensitive reagents and products were manipulated in a nitrogen atmosphere using Schlenk techniques. All solvents were purified and dried by standard procedures.[33] I.r. spectra were recorded in the region 4 000—400 cm^{-1} on a Perkin-Elmer 398 spectrophotometer. A FT-Bruker SY 200 spectrometer was used for the ^{31}P n.m.r. recordings ($CDCl_3$ solution) (positive chemical shifts are downfield relative to H_3PO_4). The u.v. spectra were recorded on a Beckman Acta CIII spectrophotometer (CH_2Cl_2 solutions).

Preparation of $[MCo_3(CO)_{12}\{\mu_3\text{-}Cu(PPh_3)\}]$ [M = Fe (**3**) *or* Ru (**4**)].—A toluene solution (10 cm^3) of $[\{Cu(PPh_3)Cl\}_4]$ (0.153 g, 0.11 mmol) was added to a suspension of (**1**)[34] or (**2**)[13] (0.41 mmol) in toluene (20 cm^3). After stirring for 1 h at room temperature, the red solution was filtered and evaporated under reduced pressure. Extraction of the solid residue with hexane gave (**3**) or (**4**). (**3**) (0.197 g, 53.7%), decomp. 170—175 °C (Found: C, 40.5; H, 1.8. Calc. for $C_{30}H_{15}Co_3CuFeO_{12}P$: C, 40.25; H, 1.70%); i.r., ν(CO) (KBr): 2 074m, 2 012vs, 1 981s, 1 972s, and 1 856s cm^{-1}; u.v., $\lambda_{max.}(CH_2Cl_2)$: 344, 416 (sh), and 552 nm; $^{31}P\text{-}\{^1H\}$ n.m.r. ($CDCl_3$): δ, 5.38 p.p.m. (**4**) (0.257 g, 66.7%), m.p. 180—182 °C (Found: C, 38.7; H, 1.7. Calc. for $C_{30}H_{15}Co_3CuO_{12}PRu$: C, 38.30; H, 1.60%); i.r., ν(CO) (KBr):

* It should be noticed that the level energies are parameter dependent. We do not find any indication of the parameters used for Cu by Evans and Mingos.[11]

† Although the $a'_1(2a_1)$ and the $a''(b_2)$ levels could mix due to the lowering of the symmetry from D_{3h} in $Co_3(CO)_9^{3-}$ to C_{3v} in $[RuCo_3(CO)_{12}\{\mu_3\text{-}Au(PH_3)\}]$ (both levels will then be of a_1 symmetry), this does not happen to an appreciable extent (the weight of one level into another is less than 1%). This allows us to add both contributions.

‡ The situation would be similar for the proton being inside the tetrahedral $RuCo_3$ unit since $a'_1(2a_1)$ would be stabilized with respect to the capped geometry but $a''_2(b_2)$ would also be destabilized. Steric factors also do not favour the proton sitting inside the tetrahedral Co_3Ru unit: for a M–H bond length of 1.734 Å (*i.e.* equal to the other Co–H bond lengths) the Ru–Co bond would then be 3.04 Å.

2 083s, 2 005vs, 1 970s, 1 884w, 1 856 (sh), and 1 850 s cm^{-1}; u.v., $\lambda_{max.}(CH_2Cl_2)$: 325, 394, and 488 nm; $^{31}P-\{^1H\}$ n.m.r. ($CDCl_3$): δ, 5.69 p.p.m.

Preparation of $[RuCo_3(CO)_{12}\{\mu_3\text{-}Au(PPh_3)\}]$ (**5**).—A diethyl ether (10 cm^3) solution of $Au(PPh_3)Cl$ (0.330 g, 0.67 mmol) was added to a suspension of $Na[RuCo_3(CO)_{12}]$ (0.420 g, 0.66 mmol) in toluene (20 cm^3). The solution became red-purple immediately. After stirring for 0.25 h at room temperature, the solution was filtered and evaporated under reduced pressure. Extraction of the solid residue with hexane gave (**5**) [form (A)] (0.055 g, 8%). The remaining solid, crystallized from dichloromethane–hexane (1:10), afforded (**5**) in the (B) form (0.485 g, 69%). (**5**) form (A), decomp. 170—180 °C (Found: C, 33.8; H, 1.6; P, 3.1. Calc. for $C_{30}H_{15}AuCo_3O_{12}PRu$: C, 33.55; H, 1.40; P, 2.90%); i.r., ν(CO) (KBr): 2 082w, 2 013vs, 1 975 (sh), 1 950 (sh), 1 900w, and 1 860vs cm^{-1}; u.v., $\lambda_{max.}(CH_2Cl_2)$: 328, 398, and 508 nm. (**5**) form (B), decomp. 160—170 °C (Found: C, 34.0; H, 1.4; P, 2.6%); i.r., ν(CO) (KBr): 2 084s, 2 041s, 2 019vs, 1 998vs, 1 903m, and 1 847vs cm^{-1}. Other data analogous to form (A).

Preparation of $[Cu(PPh_3)_3][FeCo_3(CO)_{12}]$ (**6**) *and* $[Cu(PPh_3)_3][RuCo_3(CO)_{12}]$ (**7**).—The cluster (**3**) or (**4**) (0.077 mmol) and PPh_3 (0.201 g, 0.077 mmol) was stirred in diethyl ether (20 cm^3) at room temperature for 2 h, and a violet product precipitated. The solid was filtered off, washed with diethyl ether, and dried under vacuum. (**6**) (0.050 g, 69.4% based on PPh_3), decomp. 160—165 °C (Found: C, 55.3; H, 3.4. Calc. for $C_{66}H_{45}Co_3CuFeO_{12}P_3$: C, 55.85; H, 3.20%); i.r., ν(CO) (KBr): 2 059vw, 1 995vs, 1 967m, 1 925m, 1 818m, and 1 811 (sh) cm^{-1}; u.v., $\lambda_{max.}(CH_2Cl_2)$: 370 and 510 nm; $^{31}P-\{^1H\}$ n.m.r., ($CDCl_3$): δ, 1.98 p.p.m. (**7**) (0.057 g, 76.3% based on PPh_3), m.p. 162—164 °C (Found: C, 54.2; H, 3.0. Calc. for $C_{66}H_{45}Co_3CuO_{12}P_3Ru$: C, 54.15; H, 3.10%); i.r., ν(CO) (KBr): 2 062vw, 2 011 (sh), 1 997vs, 1 965s, 1 812s, and 1 805 (sh) cm^{-1}; u.v., $\lambda_{max.}(CH_2Cl_2)$: 320 (sh), 392, and 467 nm; $^{31}P-\{^1H\}$ n.m.r. ($CDCl_3$): δ, 1.70 p.p.m.

Reaction of $K[RuCo_3(CO)_{12}]$ (**2**) *with* $[Cu(PPh_3)_2]NO_3$.—A solution of $[Cu(PPh_3)_2]NO_3$ (0.367 g, 0.565 mmol) in CH_2Cl_2 (10 cm^3) was added to a suspension of cluster (**2**) (0.370 g, 0.566 mmol) in toluene (20 cm^3). After stirring at room temperature for 1 h, the red solution was filtered and evaporated under reduced pressure. Extraction of the solid residue with hexane afforded complex (**4**) (0.120 g, 22.6% based on Ru). The recrystallization of the solid left from CH_2Cl_2–hexane afforded complex (**7**) (0.270 g, 32.6% based on Ru).

Reaction of $K[FeCo_3(CO)_{12}]$ (**1**) *with* $Cu(AsPh_3)_2Cl$.—A solution of $Cu(AsPh_3)_2Cl$ (0.156 g, 0.219 mmol) in toluene (10 cm^3) was added to a suspension of (**1**) (0.130 g, 0.214 mmol) in toluene (10 cm^3). After 0.5 h, the purple solution was filtered and evaporated under reduced pressure. Extraction of the solid residue with hexane afforded $[FeCo_3(CO)_{12}\{\mu_3\text{-}Cu(AsPh_3)\}]$ (**8**). The solid left was extracted with toluene at 40 °C, affording $[Cu(AsPh_3)_3][FeCo_3(CO)_{12}]$ (**9**). (**8**) (0.018 g, 8.9%), decomp. 165—170 °C (Found: C, 38.7; H, 1.7. Calc. for $C_{30}H_{15}AsCo_3CuFeO_{12}$: C, 38.40; H, 1.60%); i.r., ν(CO) (KBr): 2 073m, 2 005vs, 1 980 (sh), 1 971s, and 1 856s cm^{-1}; u.v., $\lambda_{max.}(CH_2Cl_2)$: 340, 395 (sh), and 548 nm. (**9**) (0.096 g, 29.5%), decomp. 175—180 °C (Found: C, 51.6; H, 3.3. Calc. for $C_{66}H_{45}As_3Co_3CuFeO_{12}$: C, 51.10; H, 2.90%); i.r., ν(CO) (KBr): 2 060vw, 1 998vs, 1 966m, 1 930m, and 1 814s cm^{-1} u.v., $\lambda_{max.}(CH_2Cl_2)$: 365 and 508 nm.

Preparation of $[Au(PPh_3)_2][RuCo_3(CO)_{12}]$ (**10**).—The cluster (**5**) (0.095 g, 0.09 mmol) and PPh_3 (0.023 g, 0.09 mmol) were stirred in diethyl ether (25 cm^3) at room temperature for 0.5 h, and a red product precipitated. The solid was filtered off, washed with diethyl ether, and dried under vacuum. Yield 92%,

Table 3. Crystal data and selected details of structure determinations

	(**4**)	(**5**)
Formula	$C_{30}H_{15}Co_3CuO_{12}PRu$	$C_{30}H_{15}AuCo_3O_{12}PRu$
M	939.83	1 073.3
Colour	Dark red	Purple
Crystal dimensions (mm)	0.10 × 0.20 × 0.24	0.20 × 0.10 × 0.10
Crystal system	Monoclinic	Monoclinic
Space group	$P2_1/m$	$P2_1/c$
a/Å	9.122(3)	8.921(3)
b/Å	15.010(6)	14.165(2)
c/Å	12.580(7)	26.72(1)
β/°	107.86(3)	91.95(4)
U/Å^3	1 639	3 374
D_c/g cm^{-3}	1.90	2.12
F(000)	920	2 040
Z	2	4
Radiation (λ/Å)	Nb-filtered Mo-K_α (0.710 69)	Mo-K_α (0.710 69)
μ(Mo-K_α)/cm^{-1}	26.75	65
θ range (min., max.)/°	3, 24	2, 30
Data collected	2 803	8 138
No. unique observed reflections	1 329	1 994
$I > n\sigma(I)$	$n = 2$	$n = 4$
R	0.049	0.058
R'	0.059	0.042
w	$0.878/[\sigma^2(F_o) + 0.015\ F_o^2]$	$2.1/\sigma^2(F_o)$

Table 4. Fractional atomic co-ordinates (× 10^4) (with e.s.d.s in parentheses) for the non-hydrogen atoms of $[RuCo_3(CO)_{12}\{\mu_3\text{-}Cu(PPh_3)\}]$ (**4**)

Atom	*X*/*a*	*Y*/*b*	*Z*/*c*
Ru	−589(2)	2 500	128(1)
Cu	1 023(2)	2 500	3 698(2)
Co(1)	1 829(2)	2 500	1 927(2)
Co(2)	−548(2)	1 665(1)	1 970(1)
P	1 609(5)	2 500	5 532(3)
O(1)	−3 998(15)	2 500	−1 165(11)
O(2)	270(14)	1 035(8)	−1 216(9)
O(3)	3 435(16)	2 500	262(13)
O(4)	4 622(16)	2 500	3 800(12)
O(5)	2 046(12)	576(8)	1 853(11)
O(6)	−504(13)	539(7)	3 859(8)
O(7)	−2 620(13)	528(7)	330(8)
O(8)	−3 373(15)	2 500	2 145(13)
C(1)	−2 721(24)	2 500	−702(15)
C(2)	−67(15)	1 562(10)	−727(10)
C(3)	2 734(21)	2 500	870(16)
C(4)	3 495(20)	2 500	3 102(14)
C(5)	1 407(14)	1 234(9)	1 900(11)
C(6)	−482(15)	1 010(10)	3 153(11)
C(7)	−1 773(14)	1 002(9)	915(10)
C(8)	−2 175(22)	2 500	2 068(15)
C(9)	−157(19)	2 500	5 959(13)
C(10)	−818(15)	1 683(9)	6 057(10)
C(11)	−2 250(18)	1 725(10)	6 311(12)
C(12)	−2 896(24)	2 500	6 399(17)
C(13)	2 702(13)	1 531(8)	6 233(9)
C(14)	3 217(16)	917(10)	5 569(11)
C(15)	4 049(19)	171(12)	6 118(13)
C(16)	4 375(18)	77(12)	7 265(13)
C(17)	3 863(18)	647(11)	7 892(13)
C(18)	2 964(16)	1 421(10)	7 392(12)

Table 5. Fractional atomic co-ordinates ($\times 10^4$) (with e.s.d.s in parentheses) for $[RuCo_3(CO)_{12}\{\mu_3\text{-}Au(PPh_3)\}]$ (**5**)

Atom	*X/a*	*Y/b*	*Z/c*	Atom	*X/b*	*Y/b*	*Z/c*
Ru	2 780(3)	−752(2)	2 044(1)	C(10)	2 700(29)	18(19)	419(11)
Au	1 816(1)	1 677(1)	972(1)	O(10)	2 985(23)	55(16)	4(8)
Co(1)	780(4)	536(2)	1 715(1)	C(11)	3 027(30)	−1 304(22)	1 176(11)
Co(2)	2 619(4)	−131(2)	1 103(1)	O(11)	3 169(19)	−2 103(13)	990(7)
Co(3)	3 536(4)	1 000(2)	1 762(1)	C(12)	343(27)	−188(18)	1 148(9)
P	1 036(7)	2 934(4)	493(2)	O(12)	−531(23)	−517(15)	883(8)
C(1)	4 855(26)	−1 287(18)	2 088(9)	C(13)	−992(24)	3 049(16)	496(8)
O(1)	5 935(22)	−1 695(17)	2 103(7)	C(14)	−1 712(25)	3 863(16)	674(8)
C(2)	1 784(28)	−1 968(20)	2 081(10)	C(15)	−3 344(27)	3 871(17)	686(8)
O(2)	1 244(25)	−2 700(16)	2 078(8)	C(16)	−4 162(25)	3 137(19)	530(9)
C(3)	2 629(26)	−598(18)	2 701(10)	C(17)	−3 485(28)	2 318(19)	372(10)
O(3)	2 602(21)	−411(14)	3 148(8)	C(18)	−1 842(26)	2 270(17)	364(8)
C(4)	−97(30)	−203(21)	2 161(11)	C(19)	1 486(22)	2 901(14)	−153(8)
O(4)	−824(23)	−622(16)	2 390(8)	C(20)	598(23)	3 412(18)	−516(9)
C(5)	−808(27)	1 271(18)	1 639(10)	C(21)	1 029(26)	3 427(20)	−1 025(9)
O(5)	−1 770(20)	1 806(15)	1 620(7)	C(22)	2 163(27)	2 885(18)	−1 163(9)
C(6)	1 852(26)	1 388(18)	2 153(10)	C(23)	2 977(27)	2 360(17)	−832(10)
O(6)	1 619(20)	1 806(15)	2 537(7)	C(24)	2 677(24)	2 355(16)	−309(9)
C(7)	4 368(27)	2 186(19)	1 667(10)	C(25)	1 720(23)	4 047(16)	724(9)
O(7)	4 719(20)	2 928(13)	1 645(7)	C(26)	1 679(28)	4 168(20)	1 293(10)
C(8)	4 796(35)	763(24)	2 246(13)	C(27)	2 420(28)	4 951(19)	1 533(10)
O(8)	5 722(25)	799(17)	2 567(9)	C(28)	3 188(26)	5 595(18)	1 216(9)
C(9)	4 747(26)	328(16)	1 242(9)	C(29)	3 346(26)	5 463(18)	661(10)
O(9)	5 863(20)	212(13)	1 107(7)	C(30)	2 608(25)	4 658(16)	435(8)

Table 6. Extended Huckel parameters for the mercury atom *

Orbital	*Hii*/eV	ζ_1	ζ_2
Hg 6*s*	−12.76	2.649	
6*p*	−6.96	2.631	
5*d*	−17.61	6.463 (0.6905)	3.032 (0.5593)

* ζ is the Slater exponent whose coefficient of the double-ζ expansion is given in parentheses.

m.p. 160—165 °C (Found: C, 43.1; H, 2.4. Calc. for $C_{48}H_{30}AuCo_3O_{12}PRu$: C, 43.15; H, 2.25%); i.r., ν(CO) (KBr): 2 015vs, 2 000vs, 1 977s, 1 964s, 1 951m, and 1 785s cm^{-1}; u.v., $\lambda_{max.}(CH_2Cl_2)$: 392 and 450 (sh) nm.

Crystal-structure Determinations.—Crystals of (**4**) and (**5**) suitable for *X*-ray analysis were obtained by slow cooling of hexane solutions at −15 °C.

Details of crystal parameters, data collection parameters, and refinement data for (**4**) and (**5**) are summarised in Table 3. The method of data collection used normal procedures previously described.[5,33] Intensity measurements were made on a Siemens AED diffractometer (θ/2θ scan mode) for (**4**) and on a Nonius CAD4 diffractometer (scan θ/scan ω = 1, scan width = 1 + 0.35 tanθ) for (**5**). All data sets were corrected for Lorentz and polarisation factors. No absorption correction was applied in view of the low absorbance of the samples. Neutral-atom scattering factors, corrected for anomalous dispersion for Au, Ru, Co, Cu, and P, were from ref. 35.

The two structures were solved by Patterson methods and refined by full-matrix least squares using the SHELX system of computer programs.[36] In (**4**), all the non-hydrogen atoms, except the carbons of the phenyl rings, were assigned anisotropic thermal parameters in the last cycles of refinement, hydrogens being placed at calculated positions in the last calculations. In (**5**), all the non-hydrogen atoms were assigned anisotropic thermal parameters. The final atomic co-ordinates for (**4**) and (**5**) are presented in Tables 4 and 5, respectively.

Computational Details.—The parameters used in the extended Hückel calculations for Co, Cu, Ru, and Au were taken from refs. 37—42. The Hg exponents were taken from ref. 40 and the *Hii*'s (see Table 6) obtained from charge iterative calculations on $Hg[Co(CO)_4]_2$ using the experimental geometry.[41] The modified Wolfsberg–Helmolz formula[42] was used throughout this work. The geometries used for the cluster calculations were somewhat idealized from the experimental ones, using for instance C_{3v} or pseudo-C_{3v} geometries for the $RuCo_3(CO)_{12}M'$ system [M' = $Au(PH_3)$, $Cu(PH_3)$, or $HgCo(CO)_4$[15]].

Acknowledgements

Financial support from the C.N.R.S. (GRECO CO), N.A.T.O. (to P. B. and A. T.), and C.N.R. is acknowledged. We also thank Johnson Matthey for a generous loan of $HAuCl_4$. Calculations were carried out at the Centre de Calcul du C.N.R.S. (Strasbourg–Cronenbourg).

References

1 P. R. Raithby, in 'Transition Metal Clusters, ed. B. F. G. Johnson, Wiley, Chichester, 1980, p. 5.
2 W. L. Gladfelter and G. L. Geoffroy, *Adv. Organomet. Chem.*, 1981, **18**, 207.
3 I. D. Salter and F. G. A. Stone, *J. Organomet. Chem.*, 1984, **260**, C71 and refs. therein.
4 P. Braunstein and J. Rose, *J. Organomet. Chem.*, 1984, **262**, 223.
5 P. Braunstein, J. Rose, A. M. Manotti-Lanfredi, A. Tiripicchio, and E. Sappa, *J. Chem. Soc., Dalton Trans.*, 1984, 1843 and refs. therein.
6 P. G. Jones, *Gold Bull.*, 1983, **16**, 114; P. Braunstein and J. Rose, *Gold Bull.*, 1985, **18**, 17.
7 R. L. Pruett and J. S. Bradley, Exxon Co. (U.S.A.), Eur. P. 37700/1981.
8 K. Wade, *Adv. Inorg. Chem. Radiochem.*, 1976, **18**, 67.
9 B. F. G. Johnson, J. Lewis, W. J. H. Nelson, P. R. Raithby, and M. D. Vargas, *J. Chem. Soc., Chem. Commun.*, 1983, 608.
10 L. J. Farrugia, M. J. Freeman, M. Green, A. G. Orpen, F. G. A. Stone, and I. D. Salter, *J. Organomet. Chem.*, 1983, **249**, 273.
11 D. G. Evans and D. M. P. Mingos, *J. Organomet. Chem.*, 1982, **232**, 171.
12 B. F. G. Johnson, J. Lewis, W. J. H. Nelson, M. D. Vargas, D. Braga, and M. McPartlin, *J. Organomet. Chem.*, 1983, **246**, C69.
13 P. Braunstein, J. Rose, Y. Dusausoy, and J. P. Mangeot, *C.R. Acad. Sci. Paris, Ser. 2*, 1982, **249**, 967.

14 P. Braunstein, J. Rose, and O. Bars, *J. Organomet. Chem.*, 1983, **252**, C101.
15 P. Braunstein, J. Rose, A. Tiripicchio, and M. Tiripicchio-Camellini, *J. Chem. Soc., Chem. Commun.*, 1984, 391.
16 P. Klufers, *Angew. Chem., Int. Ed. Engl.*, 1984, **23**, 307.
17 J. W. Lauher and K. Wald, *J. Am. Chem. Soc.*, 1981, **103**, 7648.
18 T. L. Blundell and H. M. Powell, *J. Chem. Soc. A*, 1971, 1685.
19 M. J. Freeman, M. Green, A. G. Orpen, I. D. Salter, and F. G. A. Stone, *J. Chem. Soc., Chem. Commun.*, 1983, 1332.
20 J. S. Bradley, R. L. Pruett, E. Hill, G. B. Ansell, M. E. Leonowicz, and M. A. Modrick, *Organometallics*, 1982, **1**, 748.
21 S. R. Bunkhall, H. D. Holden, B. F. G. Johnson, J. Lewis, G. N. Pain, P. R. Raithby, and M. J. Taylor, *J. Chem. Soc., Chem. Commun.*, 1984, 25.
22 O. Kahn and M. F. Koenig, 'Donnees Fondamentales pour la Chimie, Hermann, Paris, 1972, p. 22.
23 F. E. Simon and J. W. Lauher, *Inorg. Chem.*, 1980, **19**, 2338.
24 P. Braunstein, U. Schubert, and M. Burgard, *Inorg. Chem.*, 1984, **23**, 4057.
25 R. G. Teller, R. D. Wilson, R. K. McMullan, T. F. Koetzle, and R. Bau, *J. Am. Chem. Soc.*, 1978, **100**, 3071.
26 R. Hoffmann, *J. Chem. Phys.*, 1963, **39**, 1397; R. Hoffmann and W. N. Lipscomb, *ibid.*, 1962, **36**, 3179; 1962, **37**, 2872.
27 R. Hoffmann, *Science*, 1981, **211**, 995.
28 A. Dedieu and R. Hoffmann, *J. Am. Chem. Soc.*, 1978, **100**, 2074.
29 D. G. Evans and D. M. P. Mingos, *J. Organomet. Chem.*, 1982, **240**, 321.
30 J. Evans, *J. Chem. Soc., Dalton Trans.*, 1980, 1005.
31 (*a*) J. K. Burdett, *J. Chem. Soc., Faraday Trans. 2*, 1974, 1599; (*b*) M. Elian and R. Hoffmann, *Inorg. Chem.*, 1975, **14**, 1058; (*c*) D. M. P. Mingos, *J. Chem. Soc., Dalton Trans.*, 1977, 602; (*d*) P. Hofmann, *Angew. Chem.*, 1977, **89**, 551.
32 J. K. Burdett and T. A. Albright, *Inorg. Chem.* 1979, **18**, 2112.
33 R. Bender, P. Braunstein, J. M. Jud, and Y. Dusausoy, *Inorg. Chem.*, 1983, **22**, 3394.
34 P. Chini, L. Colli, and M. Peraldo, *Gazz. Chim. Ital.*, 1960, **90**, 1005.
35 'International Tables for *X*-Ray Crystallography, Kynoch Press, Birmingham, 1974, vol. 4.
36 G. M. Sheldrick, SHELX, system of computing programs, Cambridge, 1976.
37 R. H. Summerville and R. Hoffmann, *J. Am. Chem. Soc.*, 1976, **98**, 7240.
38 D. L. Du Bois and R. Hoffmann, *Nouv. J. Chim.*, 1977, **1**, 477.
39 S. Komiya, T. A. Albright, R. Hoffmann, and J. K. Kochi, *J. Am. Chem. Soc.*, 1976, **98**, 7255.
40 H. Basch and H. B. Gray, *Theor. Chim. Acta*, 1966, **4**, 367.
41 G. M. Sheldrick and R. N. F. Simpson, *J. Chem. Soc. A*, 1968, 1005.
42 J. H. Ammeter, H. B. Burgi, J. C. Thibeault, and R. Hoffmann, *J. Am. Chem. Soc.*, 1978, **100**, 3686.

Received 3rd *January* 1985; *Paper* 5/027